Transactions of the Korean Nuclear Society Virtual Autumn Meeting
December 17-18

Source Expansion Nodal Method solution for the Generalized $SP_3^{(0)}$ equations

Jorge Gonzalez-Amoros and Han Gyu Joo*
Department of Nuclear Engineering, Seoul National University
1 Gwanak-ro, Gwanak-gu, Seoul, 08826, Korea
Corresponding author: joohan@snu.ac.kr

1. Introduction

The Simplified P_n (SP_n) equations are a pseudo-transport methodology widely used nowadays in the second stage of the two-step method and commonly applied in industrial practical uses such as core design or safety assessment of nuclear reactors. The most widespread form of the equations is the SP_3 one. Its slightly higher implementation complexity and bigger computational burden is assumed as its results accuracy outperforms by far the one of the diffusion equation (SP_1). However, when Gelbard [1] first proposed the SP_n equations he did not provide the theory with boundary conditions as his example was limited to the infinite domain. This fact led to the assumption of ad hoc domain boundary conditions involving the diffusion-like first order derivatives in the surface normal direction when applied to piecewise homogeneous regions. These non-physical boundary conditions limit the virtues of the SP_n theory.

With the objective of finding a remedy to these inconsistencies as well as giving a physical basis to the theory Chao [2],[3],[4] has proposed the Generalized SP_n ($GSP_n^{(k)}$) equations. Based on the reasoning and applying the techniques employed by Davison [5],[6],[7] in his P_n theory formulation for piece-wise homogeneous regions, Chao works out a more rigorous subset of boundary conditions and a particular angular flux distribution consistent with the ones obtained by Selengut [8] in his work on the P_n theory.

The main purpose of this paper is finding a methodology that allows for the proof that the $GSP_n^{(k)}$ ($GSP_3^{(0)}$ more precisely) equations entail an improvement from the traditional SP_3 theory with its associated ad hoc 1D boundary conditions.

Thus, the solving method concluded as the most adequate to catch the potentiality of the $GSP_3^{(0)}$ equations and at the same time be easily applicable to MG problems is the Two-dimensional Source Expansion Nodal Method (2D SENM) succinctly described by Joo [9] for pin power reconstruction purposes. The most crucial point of the 2D SENM application to the $GSP_3^{(0)}$ equations is the right choice of the homogeneous flux expansion form so every term of the new rigorous boundary conditions is preserved.

In order to assess the performance of the $GSP_3^{(0)}$ equations the VERA 2D benchmark is employed.

2. The $GSP_3^{(0)}$ equations

The $GSP_n^{(k)}$ theory derivation consists of a complex mathematical development. In his papers Chao provides full detail of this derivation and therefore it will be omitted here. The final and general expression for the $GSP_n^{(k)}$ equations which is relevant for this work is the following:

$$\frac{n+k}{2n+1}\boldsymbol{F}_{n-1}^{(k)}(r)+\Sigma_n\boldsymbol{F}_n^{(k)}(r)+\frac{n+1-k}{2n+1}\nabla^2\boldsymbol{F}_{n+1}^{(k)}(r)=\boldsymbol{G}_n^{(k)}(r),\qquad n\geq k \tag{1}$$

The k in equation (1) corresponds to the layer number, the higher the number of the layer is the closer the $GSP_n^{(k)}$ equations are to the P_n ones. In this paper the equation order n is set to 3 and the layer number is kept 0 which implies equivalence to the classic SP_3 theory but with the new boundary conditions.

With regards to the scattering order, it is limited to isotropic with inflow transport correction and consequently $\Sigma_{n=1}=\Sigma_{tr}$ and $\Sigma_{n>1}=\Sigma_t$. With all these aspects considered the even moment coupled $GSP_3^{(0)}$ equations in 2D are:

$$\begin{cases}-D_0(1-\gamma)\left(\frac{\partial^2}{\partial x^2}+\frac{\partial^2}{\partial y^2}\right)F_0+\left(\frac{5}{4}\gamma^2\Sigma_t+\Sigma_0\right)F_0-\frac{75}{8}\gamma^2\Sigma_{tr}\Sigma_t^2F_2=Q_0\\ -\frac{28}{45\gamma}\frac{\Sigma_t}{\Sigma_{tr}}D_2\left(\frac{\partial^2}{\partial x^2}+\frac{\partial^2}{\partial y^2}\right)F_2-\frac{2}{15\Sigma_{tr}}F_0+\Sigma_tF_2=0\end{cases}$$
$$D_0=\frac{1}{3\Sigma_{tr}},\qquad D_2=\frac{3}{7\Sigma_t},\qquad \gamma=\frac{28\Sigma_t}{28\Sigma_t+27\Sigma_{tr}} \tag{2}$$

These equations are equivalent to the SP_3 ones. Equation (2) is employed for implementation convenience and stability but there is full correspondence between the F_n variables and the traditional ϕ_n.

The rigorous boundary conditions associated to this $GSP_3^{(0)}$ equations are as follow:

$$\Phi_{0,0}=\left(\frac{1}{4}-\frac{5}{32}\gamma\right)F_0+\frac{75}{64}\gamma\Sigma_{tr}\Sigma_tF_2-G_\phi\frac{15}{32}\frac{\partial^2}{\partial y^2}F_2$$
$$\Phi_{2,0}=\left(\frac{1}{16}-\frac{5}{32}\gamma\right)F_0+\frac{75}{64}\gamma\Sigma_{tr}\Sigma_tF_2-G_\phi\frac{15}{32}\frac{\partial^2}{\partial y^2}F_2 \tag{3}$$
$$J_{0,0}=-(1-\gamma)D_0\frac{\partial}{\partial x}F_0-\frac{35}{6}\gamma\Sigma_t^2D_2\frac{\partial}{\partial x}F_2$$
$$J_{2,0}=-\left(\frac{2}{5}(1-\gamma)-\frac{27}{70}\frac{\Sigma_{tr}}{\Sigma_t}\gamma\right)D_0\frac{\partial}{\partial x}F_0-\left(\frac{7}{3}\Sigma_t^2+\frac{9}{4}\Sigma_{tr}\Sigma_t\right)\gamma D_2\frac{\partial}{\partial x}F_2$$
$$+G_J\frac{3}{2}D_2\frac{\partial}{\partial x}\frac{\partial^2}{\partial y^2}F_2$$

Note that if G_ϕ and G_J are set to 0 these boundary conditions are equivalent to the SP_3 ones.

The partial currents in the $GSP_3^{(0)}$ theory are defined as in equation (4).

$$J^{\pm}_{n,0} = \Phi_{n,0} \pm \frac{1}{2} J_{n,0} \tag{4}$$

3. The 2D SENM

The application of the SENM to a system of two moment equations (whether it is SP_3 or $GSP_3^{(0)}$) requires the decoupling of the equations by utilizing some technique. The one chosen here is the well-known similarity transformation (like in [10]) so the system results in two diffusion-like independent equations.

The main point here is the right choice of the homogeneous flux and a more detailed description of the method is avoided here as it is already present in the references.

The homogeneous equation has a Helmholtz form and an expansion in hyperbolic functions can be performed to find the solution. As previously mentioned in the introduction, it is important to choose the most adequate expansion so that all the terms in equation (3) are conserved. Two things must be considered to make the right decision, first it is evident that the expansion must contain cross terms but at the same time be simple enough so its mathematical derivation is feasible.

In this way, the commonly used expansion with corner fluxes is avoided as its application to the $GSP_3^{(0)}$ case is too complex. The alternative is the expansion with hyperbolic functions multiplied by linear functions in the transverse direction (see equation (5)). Woo [11] demonstrated that this expansion does not deteriorate the solution when compared to the continuous corner fluxes one.

$$\begin{aligned}\phi_H(x,y) = {} & a_1 \sinh(Bx) + a_2 \cosh(Bx) \\ & + a_3 \sinh(By) + a_4 \cosh(By) \\ & + a_5 y \sinh(Bx) + a_6 y \cosh(Bx) \\ & + a_7 x \sinh(By) + a_8 x \cosh(By)\end{aligned} \tag{5}$$

The homogeneous flux expansion coefficients a_i are obtained from the node boundary conditions. The approach followed is the one-node in which the four surface-averaged incoming currents and their four first moments are employed to find the eight coefficients. The expressions of the surface fluxes and currents and their first moments at the node right surface are given by equation (6).

$$\begin{aligned}\bar{\phi}_x &= \int_{-h_y/2}^{h_y/2} \phi(\frac{h_x}{2}, y)dy, & \bar{J}_x &= -D \int_{-h_y/2}^{h_y/2} \frac{\partial}{\partial x}\phi(\frac{h_x}{2}, y)dy \\ \phi_x &= \int_{-h_y/2}^{h_y/2} \omega(y)\phi(\frac{h_x}{2}, y)dy, & J_x &= -D \int_{-h_y/2}^{h_y/2} \omega(y)\frac{\partial}{\partial x}\phi(\frac{h_x}{2}, y)dy\end{aligned} \tag{6}$$

The weighting function employed for the first moment variables is the step function described in equation **Error! Reference source not found.**.

$$\omega(y) = \begin{cases} -1 & for \;\; y < 0 \\ 1 & for \;\; y \geq 0 \end{cases} \tag{7}$$

3.A. G_J term analysis

Before starting the assessment on the $GSP_3^{(0)}$ equations, however, it must be pointed out that the introduction of the second moment current leakage in equation (3) provokes instabilities in the calculations.

By manipulating G_J reached the conclusion that this value can have a considerable impact in the final result. The optimal value of this factor is determined by carrying out a series of sensitivity analysis with assemblies 5 and 6 of VERA.

For this analysis the GCs are pin homogenized with an eight groups MG structure. The GCs are generated with the MOC code NTRACER from heterogeneous 47 groups SA calculations with reflective boundary conditions. The reference result is also obtained from NTRACER with the same eight group pin-wise GCs and a 32x32 mesh per pin.

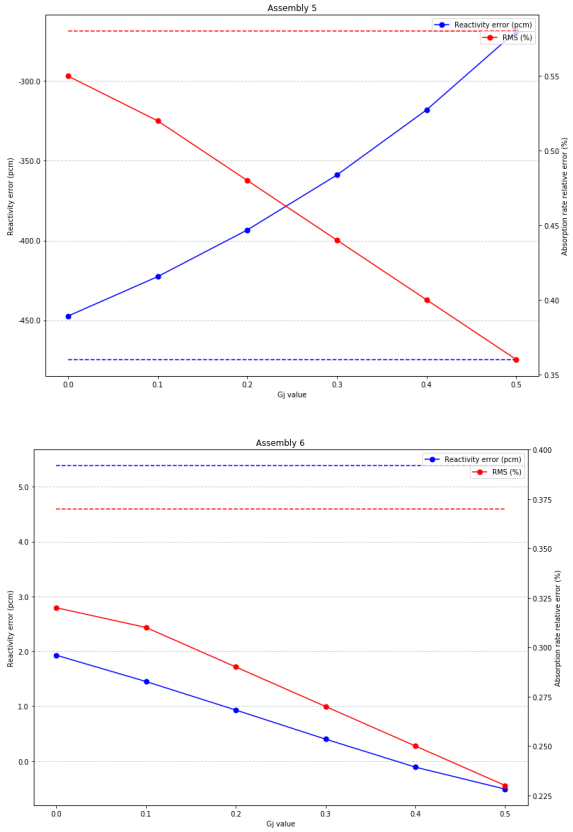

Figure 1. G_J factor sensitivity with VERA benchmark assemblies. SP3 results in dashed line.

The results depicted in Figure 1 and allow to conclude that the optimal value for G_J is 0.5 as it offers the best results for reactivity and absorption rate RMS error before the calculation starts diverging. This 0.5 value is kept in the following for the $GSP_3^{(0)}$ equations evaluation.

3.B. Mesh refinement evaluation

In order to evaluate the optimal mesh refinement for the 2D SENM solution for a fair comparison between SP_3 and $GSP_3^{(0)}$ the same VERA assembly problems are calculated with decreasing mesh sizes. The maximum mesh size that guarantees a virtually zero discretization error is then chosen for a more thorough assessment of the theory.

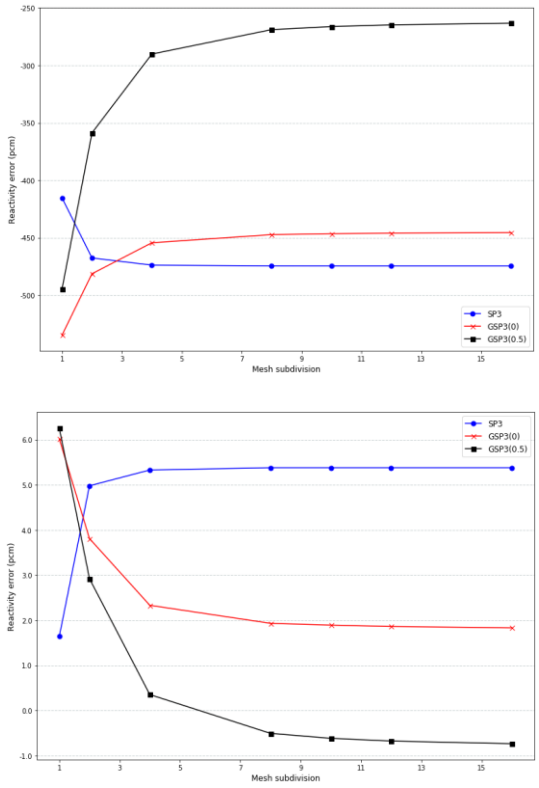

Figure 2. Reactivity error evolution with mesh refinement assembly 5 (top) and 6 (bottom).

Figure 2 shows that the 2D SENM is able to reach a negligible discretization error when an 8x8 mesh per pin is employed.

4. $GSP_3^{(0)}$ assessment

For a more thorough study the rest of VERA assemblies are calculated. The discretization achieved for SA is of 8x8 which has already been demonstrated to be fine enough to diminish the spatial discretization error. As for the NTRACER reference the node subdivision is set to 32x32 per pin.

Figure 3 shows the results for the VERA benchmark 10 assemblies. For very homogeneous cases such as assemblies 1, 2 and 6 the discretization and the transport errors are of the same order of magnitude. This fact produces that, due to error compensation, the SP_3 results might show little difference to the $GSP_3^{(0)}$ ones. However, when heterogeneities are introduced the discretization error is negligible in comparison with the transport one and an incontestable superiority of $GSP_3^{(0)}$ is observed.

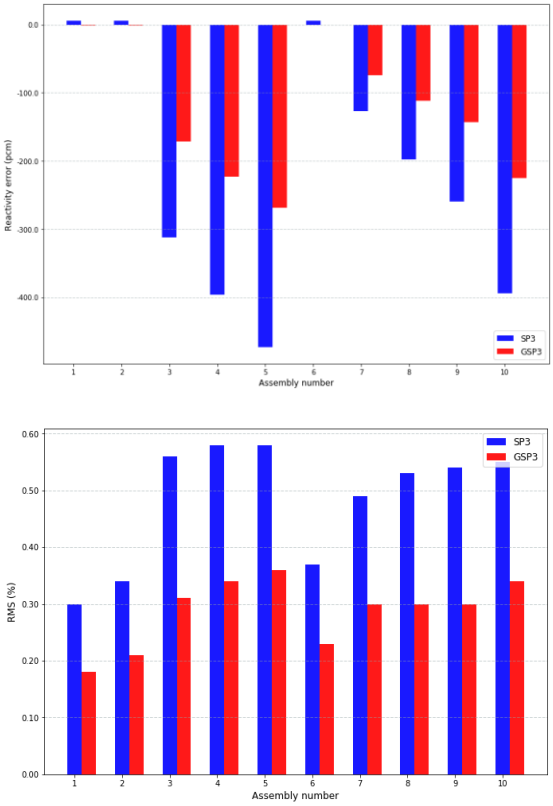

Figure 3. VERA benchmark assemblies reactivity error (top) and RMS absorption rate relative error (bottom).

For a more realistic problem the VERA 2D quarter core benchmark is calculated. Two different core states are simulated, one with all the control rods (CRs) out (ARO) and one with CR bank D inserted (benchmark problem 5). As it is a big problem he node subdivision is 2x2 and the NTRACER reference discretization is set to 16x16 per pin.

Table I summarizes the results for the core calculations. For both problems $GSP_3^{(0)}$ improves SP_3. In the core with bigger flux gradients (problem 5) improvements of up to 20 % in reactivity error and more than a 50 % in pin power RMS relative error are observed.

Table I: Results for VERA core 8G 2DSENM calculation

Discretization		2x2	
Control rods		ARO	5
SP3	Δρ (pcm)	-170.27	-198.24
	Max. (%)	1.26	3.69
	Min (%)	-1.41	-3.96
	RMS (%)	0.48	0.93
GSP3	Δρ (pcm)	-134.03	-158.15
	Max. (%)	0.52	0.95
	Min (%)	-1.27	-2.96
	RMS (%)	0.40	0.42

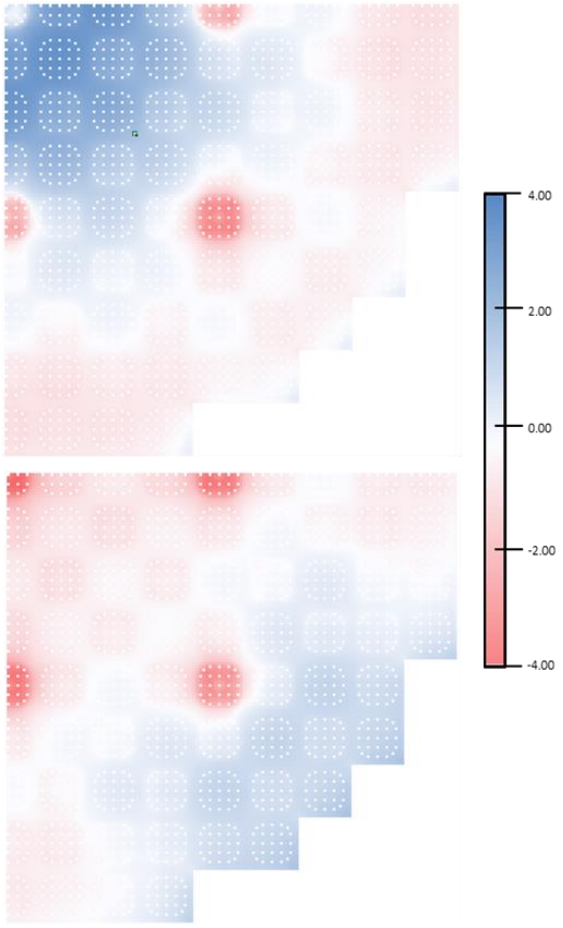

Figure 4. Pin power error (%) distribution for 8G 2DSENM calculation of VERA Problem 5 core with SP_3 (top) and $GSP_3^{(0)}$ (bottom).

5. Conclusions

The 2D SENM has been proved to be an optimal solving method to reduce the discretization error. This allowed the quasi isolation of the transport error so that the pre-eminence of the $GSP_3^{(0)}$ theory over the SP_3 one could be assessed.

Besides the homogeneous flux expansion employed here allowed the conservation of the transverse leakage terms of the rigorous $GSP_3^{(0)}$ boundary conditions. The alleged incapacity of this homogeneous flux expansion to handle the current gradient forced the introduction of a tuning factor. This tuning factor or G_J offers the best performance when set to 0.5

REFERENCES

[1] Gelbard, E. M., 1960. Application of spherical harmonics method to reactor problems. Bettis Atomic Power Laboratory, West Mifflin, PA, Technical Report No. WAPD-BT-20.
[2] Chao, Y.-A., 2016. A new and rigorous spn theory for piecewise homogeneous regions. Annals of Nuclear Energy 96, 112-125.
[3] Chao, Y.-A., 2017. A new and rigorous spn theory{part ii: Generalization to gspn. Annals of Nuclear Energy 110, 1176-1196.
[4] Chao, Y.-A., 2018. A new and rigorous spn theory-part iii: A succinct summary of the gspn theory, the p3 equivalent gsp3 (3) and implementation issues. Annals of Nuclear Energy 119, 310-321.
[5] Davison, B., 1957. Neutron transport theory.
[6] Davison, B., 1958a. Neutron transport theory. Clarendon Press.
[7] Davison, B., 1958b. Spherical-harmonics method for neutron transport theory problems with incomplete symmetry. Canadian Journal of Physics 36 (4), 462-475.
[8] Selengut, D., 1970. A new form of p3 approximation. In: TRANSACTIONS OF THE AMERICAN NUCLEAR SOCIETY. Vol. 13. SPRINGER VERLAG 175 FIFTH AVE, NEW YORK, NY 10010, p. 625.
[9] Joo, H. G., Yoon, J. I., Baek, S. G., 2009. Multigroup pin power reconstruction with two-dimensional source expansion and corner flux discontinuity. Annals of Nuclear Energy 36 (1), 85-97.
[10] Bahabadi, M. H. J., Pazirandeh, A., Athari, M., 2015. New analytic function expansion nodal (afen) method for solving multigroup neutron simplified p3 (sp3) equations. Annals of Nuclear Energy 77, 148-160.
[11] Woo, S. W., Cho, N. Z., Noh, J. M., 2001. The analytic function expansion nodal method refined with transverse gradient basis functions and interface flux moments. Nuclear science and engineering 139 (2), 156-173.